

CRYSTAL STRUCTURE OF MISERITE, A ZOLTAI TYPE 5 STRUCTURE

J. DOUGLAS SCOTT*

Department of Geological Sciences, Queen's University, Kingston, Ontario K7L 3N6

ABSTRACT

Miserite is triclinic, space group $P\bar{1}$, a 10.100(5), b 16.014(7), c 7.377(5) Å, α 96°25(3)', β 111°9(3)', γ 76°34(2)'. Its crystal structure has been refined to $R=0.062$ for 2755 observed reflections. It is characterized by the presence of three-membered sub-chains of silica tetrahedra, similar to those of wollastonite, but having all tetrahedra sharing three corners. Four such sub-chains link to produce a closed quadruple $Si_{12}O_{30}$ chain composite, infinite in extent parallel to c , and centred on each cell corner in [001] projection. These pipes display almost perfect mmm symmetry and are cross-linked parallel to a by K atoms, adjacent pipes being displaced vertically by exactly $c/2$. Edge-sharing columns of Ca polyhedra bonded to each other and to independent Si_2O_7 groups form a slab infinite in extent in a and c , which falls between the pipes and connects them in the b direction.

The ideal formula for miserite is $KCa_8\Box(Si_2O_7)(Si_6O_{18})(OH)F$, with $Z=2$. In the miserite studied, from the Kipawa Lake area, Temiscamingue Co., Quebec, an octahedrally-coordinated virtual site defined by the slab acts as a selective structural trap for yttrium, rare earths and other minor atomic species. In addition, two empty sites within the corner pipes are capable of zeolitically sorbing both large cations and either H_2O or F at centres of symmetry located on the pipe axis with the restriction that the empty origin site is anion-specific.

Miserite is the first known representative of a Zoltai Type 5 structure.

SOMMAIRE

La misérite appartient au groupe spatial triclinique $P\bar{1}$ avec a 10.100(5), b 16.014(7), c 7.377(5) Å, α 96°25(3)', β 111°9(3)', γ 76°34(2)'. Sa structure cristalline a été affinée jusqu'au résidu $R=0.062$, sur 2755 réflexions observées. Quatre chaînes secondaires triples de tétraèdres Si-O (semblables à celles de la wollastonite, mais dont chaque tétraèdre partage trois sommets) s'unissent en une chaîne complexe $Si_{12}O_{30}$, formant un cylindre infini allongé suivant c . Ces cylindres (ou cheminées) sont centrés aux quatre coins de la maille projetée parallèlement à [001]; ils possèdent une pseudo-symétrie mmm presque parfaite; ils sont reliés l'un à l'autre en direction a par des atomes K, les deux cylindres voisins étant décrochés verticalement de $c/2$ rigou-

reusement. Des colonnes de polyèdres de coordination de Ca à arêtes communes, liés les uns aux autres ainsi qu'à des groupements indépendants Si_2O_7 , constituent dans le plan ca une plaque infinie qui vient se placer entre les cylindres et les relie en direction b .

La formule idéalisée de la misérite, pour $Z=2$, s'écrit $KCa_8\Box(Si_2O_7)(Si_6O_{18})(OH)F$. Dans la misérite étudiée, qui provient de la région du lac Kipawa, comté de Témiscamingue, Québec, une lacune à coordination octaédrale que définit la plaque joue le rôle de piège structural sélectif pour l'yttrium, les terres rares et autres espèces atomiques mineures. En outre, deux lacunes à l'intérieur des cylindres sont capables de capter, par sorption zeolitique, les cations de grande taille, ainsi que H_2O ou F, aux centres de symétrie situés sur l'axe du cylindre, ce à quoi la spécificité anionique du site vacant de l'origine impose une restriction.

La structure de la misérite nous fournit le premier représentant du type 5 de Zoltai.

(Traduit par la Rédaction)

INTRODUCTION

The complex silicate miserite has long been considered a problem mineral among researchers who have studied it. From its first erroneous identification as natroxonotlite (Williams 1891), it has been characterized by disparate analyses and formulae. Since the work of Schaller (1950), it has been classified as a K,Ca-silicate; however, all known analyses also show numerous minor elements in extremely variable proportions. Especially notable in this respect is the rare-earth content, which usually includes yttrium, cerium and lanthanum. Miserite from the type locality at Potash Sulfur Springs, Arkansas, also contains significant amounts of niobium (C. Milton*). Among other elements, the amount of fluorine reported in analyses is highly variable, especially since it may frequently be included in the high-temperature ignition loss and reported as water.

Miserite at Potash Sulfur Springs is associated with aegirine and orthoclase, and occurs as compact masses of long fibres intergrown with wollastonite (Schaller 1950). Miserite has also been reported in a variety of associations

*Present address: CANMET, 300 Lebreton St., Ottawa K1A 0G1.

*Unpublished data communicated to L. G. Berry.

from several Russian localities, where it is universally accompanied by aegirine, frequently by orthoclase, and rarely by wollastonite or pectolite. Miserite from the Kipawa carbonatite, Quebec, occurs in very coarsely crystallized form, and is not apparently associated with wollastonite or orthoclase (Berry *et al.* 1971), although it is intergrown with aegirine, agrellite and eudialyte. Most recently, miserite has been identified from Wausau, Wisconsin, where it occurs associated with aegirine and two new minerals (S. Guggenheim, pers. comm.).

Formulae were originally assigned to miserite on the basis of a wollastonite-type structure, given the association at the type locality, the variable compositions reported, and the lack of unit-cell data. Schaller (1950) first described and named miserite from Potash Sulfur Springs, recognizing it as identical to Williams' (1891) natroxonotlite (pink wollastonite) and discrediting the earlier name as "glaringly false in significance." The formula assigned by Schaller is $\text{KCa}_2\text{Si}_5\text{O}_{13}(\text{OH})_3$, and this has been used as a model for many subsequent formulae. Reports of miserite from various Russian localities in central Asia leave little doubt that the material is very similar to that found in Arkansas (Ryzhov & Moleva 1960; Kupriyanova & Vasileva 1961; Kozlova 1962; Ulyanova & Ilinski 1964; Kravchenko & Bykova 1967; Arkhangel'skaya 1968). The best description in English of the Russian material is that of Ryzhov & Moleva (1960), who compare miserite from the Alay Range (Kirgiz S.S.R.) with the Arkansas miserite, giving the formula $(\text{K},\text{Na})\text{Ca}_4\text{Si}_5\text{O}_{13}(\text{OH},\text{F})_3$. Ulyanova & Ilinski (1964), however, assign a pectolite-type formula, $\text{KCa}_2[\text{Si}_5\text{O}_8\text{OH}]$, to miserite from the same area. Other research on Russian miserite (Kupriyanova & Vasileva 1961; Kravchenko & Bykova 1967) revealed that Schaller's (1950) formula was not compatible with more accurate analyses of the Russian material, and new formulae were proposed, based on the radicals Si_6O_{17} (xonotlite-type) and $\text{Si}_6(\text{O}_{15},\text{F})$, respectively. For miserite at Kipawa, Quebec, Berry *et al.* (1971) simplified the formula, returning to a wollastonite model. They were able for the first time to determine a unit cell for the mineral which, together with their more accurate density determinations, led to a proposed formula of $16[\text{Ca},\text{K},\text{Na},\text{Al},\text{Y},\text{etc.}]\text{SiO}_3$ for the cell content, implying a structure analogous to that of wollastonite with severe disorder in the Ca site.

Previous to the Kipawa discovery, no miserite had been found in crystals suitable for a structure determination. The Arkansas type material is intergrown with wollastonite on too fine a

scale to be separated into suitable crystal fragments (M. Mrose, pers. comm.). Since cell parameters have not been reported for any miserite from Russian localities, evidently it too is not crystallized well enough for structural work. Because of the availability of relatively large quantities of well-crystallized material from Kipawa, structural studies of miserite were begun at Queen's University in 1970, at the instigation of Dr. L. G. Berry.

ANALYTICAL

A suite of miserite-containing specimens from Kipawa was collected for the Royal Ontario Museum in the early 1960's by D. C. Harris and G. Pawlick. The most coarsely crystallized of these (#M27167) was selected by Dr. L. G. Berry for all subsequent work. Coarse crushing of a portion of the largest miserite crystal permitted the removal of minor intergrown aegirine and eudialyte, and yielded pure crystalline cleavage fragments up to 3 mm in length. In view of the problematic analytic history of miserite, detailed compositional analyses were made before proceeding with structural studies.

Given the analysis of Berry *et al.* (1971) as a guide, it was possible to make a more representative selection of microprobe standards than had been used previously. Results of the new analyses (Table 1) were generally in good agree-

TABLE 1. ANALYTICAL DATA FOR KIPAWA MISERITE

Oxide	Wt. %	Atoms	Oxide	Wt. %	Atoms
SiO_2	50.18	15.92	Pr_6O_{11}	0.21	0.02
CaO	31.00	10.54	Nd_2O_3	0.86	0.10
K_2O	5.58	2.26	EuO	0.04	(0.00)
Na_2O	0.81	0.50	Dy_2O_3	0.58	0.06
MgO	0.37	0.18	Er_2O_3	0.31	0.03
MnO	0.45	0.12	Tm_2O_3	0.03	(0.00)
FeO	0.14	0.04	Yb_2O_3	0.47	0.05
Al_2O_3	0.60	0.22	Lu_2O_3	0.04	(0.00)
Y_2O_3	3.34	0.56	F	2.04	2.04
La_2O_3	0.59	0.07	H_2O	0.55	0.55
Ce_2O_3	1.00	0.11		99.19	
Ideal Formula: $\text{KCa}_5\text{Si}_7(\text{Si}_6\text{O}_{15})(\text{OH})\text{F}$					

ment with those reported in their paper. Elements formerly detected by wet-chemical methods but not by microprobe (Mg and Al) were confirmed. Two elements analyzed repeatedly with special care were K and Y, and the new values obtained approximate an average of those given previously. Microprobe results for the minor rare-earth content are in excellent

agreement with the reported wet-chemical values. Since it was considered that, for very low concentrations, wet chemistry is probably more accurate than the microprobe, all such values were accepted as given by Berry *et al.* (1971). Minor elements found in miserite from other localities, such as Nb, Ti and Sr, were searched for but not detected.

The corrected analytical sum for this new composite analysis was 96.6 wt.%, somewhat lower than ideal. Since a common feature of all recent analyses of miserite from localities other than Kipawa was the presence of fluorine, an improved method of fluorine and chlorine analysis for silicate minerals (S. Haynes, pers. comm.) was applied to 500 mg of miserite. This returned values of 2.04 wt.% F and approximately 12 ppm Cl. This in turn raised questions about the high-temperature ignition loss of 1.15 wt.% reported by Berry *et al.* (1971). Several runs were made at lower temperatures on finely-crushed 100-mg samples; all agreed closely with an H₂O content of 0.55 wt.%, bringing the final analytical sum for the Kipawa miserite to 99.19 wt.%.

Since the present analysis for Kipawa miserite was slightly different from that reported previously, a new density determination was made. Ten optically homogeneous grains weighing 15 to 25 mg were selected from the crushed material, and replicate densities were determined using a Berman balance with toluene as flotation agent. The average of these determinations was exactly the same as the previously reported value, 2.926(2) gcm⁻³, with a range of 2.924 to 2.930.

The grains used in the density determinations were then crushed and used to prepare powder-diffraction specimens for both large-camera and diffractometer work. In making the diffractometer traces, both silicon powder and a local

TABLE 2. INDEXED POWDER DATA FOR MISERITE

Kipawa					Arkansas*		
I _{obs}	d _{obs}	d _{calc}	I _{calc} [†]	hkl	I _{obs}	d _{obs}	d _{calc}
100	15.42	15.57	100	010	W	17.3	15.55
			6	110	VW	8.735	8.776
5	7.775	7.784	6	020	VWV	7.932	7.775
5	7.266	7.295	6	-110			
10	5.193	5.189	8	030	W	5.172	5.233
10	5.018	4.985	8	130			
45	4.681	4.691	27	210	S	4.638	4.693
5	4.594	4.608	6	200			
8	4.374	4.383	8	220	VWV	4.408	4.388
15	4.175	4.168	9	-130	VW	4.150	4.158
35	3.887	3.892	23	040	W	3.893	3.887
50	3.469	3.471	33	-1-22	VS	3.445	3.443
45	3.357	3.352	28	211	VS	3.339	3.342
80	3.179	3.177	74	-122			
80	3.166	3.169	74	-1-32			
90	3.140	3.141	84	310	VVS	3.144	3.140
64	3.106	3.113	56	050			
60	3.100	3.109	50	022	VS	3.090	3.090
55	3.072	3.073	47	300			
57	2.922	2.922	54	330			
25	2.873	2.870	22	250	VS	2.870	2.873
55	2.825	2.825	46	032	VS	2.800	2.812
40	2.776	2.780	44	-150			
45	2.677	2.675	44	-320	S	2.663	2.670
5	2.641	2.644	6	160			
40	2.509	2.511	26	1-11	W	2.481	2.501
5	2.454	2.456	7	350			
65	2.377	2.377	49	-4-12	S	2.373	2.374
5	2.352	2.365	6	-250			
8	2.346	2.351	6	410			
10	2.304	2.304	10	400	VWV	2.301	2.303
8	2.289	2.289	6	430			
			6	-152	VWV	2.242	2.241
5	2.227	2.224	6	070			
2	2.220	2.222	3	360			
4	2.195	2.200	5	-340			
			3	152	VW	2.159	2.162
43	2.103	2.102	22	0-62	S	2.097	2.098
40	1.968	1.970	18	322	S	1.964	1.963
35	1.922	1.922	16	332	VW	1.910	1.916
60	1.845	1.844	40	-2-14	VS	1.832	1.828
			4	352	VW	1.761	1.760
			2	-520	VWV	1.715	1.713
66	1.667	1.667	40	-2-92	S	1.667	1.666
20	1.641	1.642	13	-182			
			2	541	VW	1.620	1.620
50	1.589	1.585	24	-542	S	1.579	1.582
10	1.564	1.563	8	630	VW	1.555	1.564

*Data for miserite from Potash Sulphur Springs, Arkansas (C. Milton); d_{calc} from newly refined cell (Table 3).

†Calculated using POWD-5 (Clark *et al.* 1973) on the basis of the refined structure.

fluorite standard were used as internal standards in separate runs. The low-angle portion of the powder pattern for Kipawa miserite, containing all the strong lines which could be indexed exactly, is given in Table 2, together with that obtained for miserite from Arkansas by

TABLE 3. CRYSTAL DATA FOR MISERITE

	Kipawa ¹	Arkansas ²	Yakutia ³	Central Asia ⁴	Talassk Range ⁵
<i>a</i>	10.100(5)Å	10.101(7)	10.076(30)	9.96(5)	9.98(4)
<i>b</i>	16.014(7)	16.003(7)	15.998(33)	15.87(7)	16.00(7)
<i>c</i>	7.377(5)	7.310(7)	7.329(24)	7.33(4)	7.46(3)
α	96°25(3)'	96°19(4)'	96°31(16)'	95°45(24)'	95°41(33)'
β	111°9(3)'	111°8(4)'	111°21(17)'	110°52(24)'	111°5(19)'
γ	76°34(2)'	76°25(3)'	76°10(13)'	76°25(29)'	76°54(23)'
<i>v</i>	1081.88(80)Å ³	1070.90(1.11)	1067.93(3.93)	1052.57(5.75)	1083.29(5.45)
<i>D</i> _{meas}	2.926(2)	2.899	2.873	2.84	2.877
[R.E. (wt.%)	7.47	2.29	0.48	0.0	4.00
<i>Z</i>	2				
Space Group	<i>P</i> 1̄				
μ_{λ} (CuK α)	227 cm ⁻¹				

¹Present study; ²C. Milton; ³Kravchenko & Bykova (1967); ⁴Ryzhov & Moleva (1960); ⁵Kozlova (1962)

C. Milton. The powder pattern for the Kipawa miserite was indexed on the basis of Weissenberg photographs, and the resulting refined unit cell is given in Table 3. When the powder data of Milton were indexed to conform with the Kipawa pattern, it appeared to be in substantial agreement with the latter. Using these known indices, refined unit cells were calculated for the Arkansas material and for material from those Russian localities for which suitable published powder data exist (Table 3). In spite of variations in analytical content for miserite from different localities (Table 4), the unit cells as calculated are all in fairly good agreement.

TABLE 4. REDUCED ANALYSES AND POSTULATED SITE OCCUPANCIES FOR MISERITE

Element	Kipawa	Arkansas	Yakutia	Central Asia	Talassk Range
	Atoms	Atoms	Atoms	Atoms	Atoms
Si	15.92	15.31	15.69	14.74†	14.93†
Al	0.22		0.87	0.07	0.49
Ca	10.54	11.25	10.26	11.62	11.20
K	2.26	2.41	2.39	2.47	2.16
R.E.	1.00	0.77	0.05		0.66
Y*	0.84	0.51	1.38	0.89	1.20
F	2.04	2.06	2.92	0.85	4.27††
O**	46.01	46.10	45.68	47.30	47.24
Site					
X	2	2	2	<2	2
Z	0.8	0.4	0.6	0.5	0.6

Framework cell content: $K_2Ca_{10}Si_{16}O_{48}(OH,F)_8$

* Y = sum of all minor atomic species other than R.E.

** Does not include zeolitic H_2O .

† Most Russian analyses are slightly silicon-deficient for unknown reasons.

†† This value is either erroneous or indicates zeolitically trapped F.

EXPERIMENTAL

A sharp pseudo-tetragonal prism, seen to be free of twinning under the polarizing microscope, was selected for subsequent data collection. The prism faces of the rod were well-developed cleavage faces, and one terminal face appeared to be a true crystal face, later determined to be (001); the opposite end, however, was a relatively smooth, arbitrary fracture surface. It should be noted that the cleavage directions as given by Berry *et al.* (1971) are inverted, and correctly read {010} perfect and {100} imperfect.

Crystal dimensions (Table 5) were measured

TABLE 5. CRYSTAL DIMENSIONS USED FOR ABSORPTION CORRECTION

Face	d from a common origin (cm)
100	0.0052
100	0.0052
010	0.0052
010	0.0052
001	0.0622
132	0.0035

before mounting the fragment on its terminal crystal face to rotate about the prism axis. Weissenberg and precession photographs taken in this orientation enabled the calculation of indices for all bounding planes. The index (132) was assigned to the fracture surface after least-squares calculations showed it to be the simplest index approximating the actual plane.

Multiple-film Weissenberg packs for levels $hk0$ through $hk6$ were taken on a Stoe integrating camera using Ni-filtered $CuK\alpha$ radiation. Precession films of levels $h0l$ and $0kl$ and Weissenberg levels $0kl$ were used to put the data on a single overall scale. All films were read on a split-beam densitometer, and the raw intensities were corrected for Lorentz and polarization effects and for α_1 - α_2 splitting (both members of a doublet being measured wherever possible). A local version of the Hamilton-Rollett-Sparks interscale program (Hamilton *et al.* 1965) was used to reduce the data to 3389 independent reflections ($R_{scale} = 0.026$). Of these, 634 reflections were classified as unobserved and included at half the average film transmittance at the reflecting position. All reflections were corrected for absorption using the analytic program ABSCOR (Alcock 1970); transmission factors ranged from 0.28 to 0.56. Unobserved reflections were coded as less-thans and not included in the subsequent refinement. A Wilson plot of the corrected data set gave an overall temperature factor of 1.55\AA^2 , and E -statistics unambiguously indicated a centric structure in space group $P\bar{1}$. As a point of caution, it is easy to mistake [101] for the principal direction [100], since as a matter of coincidence the two vectors have identical lengths in miserite; choosing [101] would result in a close approximation of a centred monoclinic cell rather than the correct triclinic cell. Zero-level Weissenberg photographs taken in either orientation are essentially the same; however, upper-level photographs about [101] cannot be indexed on rational axes.

STRUCTURE DETERMINATION AND REFINEMENT

A three-dimensional Patterson map showed evidence of extreme peak overlap, especially around the origin, and failed to define any part of the structure clearly. An early source of confusion was the anticipation that the heaviest atom would occupy a centre of symmetry, based on the fact that the rare-earth content coincidentally equals exactly one atom in the unit cell (Table 4). However, attempts to locate such a composite atom at a centre of symmetry could not be reconciled with the Patterson ($R \approx 0.55$).

Both vector-search and direct methods were tried, but none of the major program systems available in the early 1970's appeared capable of producing a structure which could be refined. The correct structure was approached several times, but no partial structure found would refine below $R=0.29$ or produce an unambiguous difference map.

The 1973 version of MULTAN (Germain *et al.* 1971) successfully phased all 435 E -values greater than 1.5, yielding an absolute figure of merit of 1.23 and a residual of 26.1, the highest and lowest such values obtained from any run to date. An E -map revealed what subsequently proved to be the entire structure; at the conclusion of refinement all but two phases assigned by MULTAN-73 were found to have been correct. Vectors between high peaks on the E -map correlated well with peaks on the Patterson map. The seven highest peaks on the E -map were therefore assigned to Ca for an initial refinement cycle. However, refinement of these positions, together with those of two silica tetrahedra which could also be seen on the E -map, would not reduce R below 0.29. A difference map computed at this stage proved impossible to interpret, but did indicate that several of the heavy-atom assignments were definitely incorrect. It was therefore decided to abandon the traditional heavy-atom approach for this structure.

The two silica tetrahedra already found on the E -map were well-resolved and positioned approximately in the centre of the cell, and it was postulated that O atoms belonging to these tetrahedra would form part of a polyhedral framework for the heavier cations. Previous workers had characterized miserite as a pyroxenoid having a structure related to that of wollastonite (Kupriyanova & Vasileva 1961; Ulyanova & Ilinski 1964). The theory that miserite would have three-member tetrahedral chains very similar to those of wollastonite was supported by the fact that miserite has an elongation axis of 7.38\AA . This was sufficiently close to the 7.32\AA repeat unit in wollastonite, which is controlled by such chains (Prewitt & Buerger 1963), that attempts were made to extend the two known silica tetrahedra into similar chains. When these proved unsuccessful, a special program, FINDOX (available from the author on request), was written to locate poorly resolved oxygen atoms in the E -map on the basis of tentatively assigned Si sites, in the hope of mapping the expected chains. It was immediately obvious that the previously located tetrahedra represented parts of two isolated Si_2O_7 groups, related by the centre of symmetry

at $\frac{1}{2}, \frac{1}{2}, \frac{1}{2}$. Potential Si sites were then chosen from among the intermediate peaks of the E -map, and a chain pattern was rapidly resolved, resulting in the location of all remaining O atoms in the silica framework. K and Ca sites could now be correctly identified from their coordination polyhedra (RE being treated as Ca for the purpose of refinement). In two cycles of least-squares refinement with isotropic temperature factors, R fell to 0.18 for an asymmetric unit content of $\text{KC}_{20}\text{Si}_8\text{O}_{22}$.

A difference map for this trial structure showed that all K, Si and O sites were basically correct in both position and occupancy. One of the Ca sites, however, was significantly underoccupied, and there were two extra strong peaks in general positions as well as weaker peaks at two of the centres of symmetry. The underoccupied Ca site was reassigned to yttrium (and RE) with half occupancy. The two peaks in general positions were assumed to represent O(H) and F, given that reducing the analysis (Table 1) to elements yields 46.01 O atoms whereas only 44 are required by the silica tetrahedra. The two occupied centres of symmetry were accounted for by placing a half-occupied H_2O oxygen at the origin and the excess $\text{Ca}+\text{K}$ (shown in the analysis) at $0, 0, \frac{1}{2}$. Three further cycles, run with anisotropic thermal parameters for K, Ca and Si, and isotropic oxygens, reduced R to 0.089; the associated difference map indicated that all atom assignments were correct except for the rare-earth site.

Occupancy parameters and scattering factors were adjusted in numerous subsequent cycles of refinement. The origin site (designated as W) was finally assigned to an H_2O oxygen with 0.53(4) occupancy; the $0, 0, \frac{1}{2}$ site (designated as Z), to a combination of $0.54(2)\text{Ca}+0.26(3)\text{K}$; and the rare-earth site (designated as X), to all other minor elements. If 0.08 Al (total Al=0.22 atoms) is included with the Si to produce exactly 16(Si,Al), the sum of all minor atom species becomes 1.98. A composite analytic scattering-factor curve for this mixture, derived by non-linear least-squares methods, was used to refine the X -site parameters. The resulting occupancy of 1.002(3) gave a perfectly flat difference map in the region of that atom. Refinement of Si occupancies in search of the small amount of Al postulated above was less successful because of high parameter correlations; there were, however, strong indications that the Al was concentrated in Si(4) and Si(7), as might be expected from the slightly longer average bond lengths for these tetrahedra. Both these sites occur in the same chain, and probably account for slightly larger inter-tetrahedral angles in

TABLE 6. FRACTIONAL COORDINATES AND ISOTROPIC TEMPERATURE FACTORS FOR MISERITE

Site	x	y	z	B(\AA^2)
Z	0.0	0.0	0.5	1.22(10)
K	0.32021(29)	0.99315(18)	0.15955(44)	1.46(6)
X	0.00757(16)	0.60253(10)	0.15005(24)	1.72(4)
Ca 1	0.40066(21)	0.26328(14)	0.51548(31)	1.13(5)
Ca 2	0.40829(21)	0.25742(13)	0.02070(29)	0.83(5)
Ca 3	0.36304(22)	0.61689(14)	0.07902(31)	1.16(5)
Ca 4	0.00483(21)	0.40187(12)	0.34005(33)	1.04(5)
Ca 5	0.64636(22)	0.38063(14)	0.40674(31)	1.13(6)
Si 1	0.28670(27)	0.44355(17)	0.29577(39)	0.77(8)
Si 2	0.71369(27)	0.55740(17)	0.27878(39)	0.77(6)
Si 3	0.70028(34)	0.90456(20)	0.32885(49)	0.73(6)
Si 4	0.61346(27)	0.10334(17)	0.33692(39)	0.74(7)
Si 5	0.76951(26)	0.18751(17)	0.14196(40)	0.69(6)
Si 6	0.90073(17)	0.81847(18)	0.11888(39)	0.84(6)
Si 7	0.23322(31)	0.80826(21)	0.28475(44)	0.75(5)
Si 8	0.09730(34)	0.18089(22)	0.30029(49)	0.68(7)
O 1	0.12345(90)	0.45144(66)	0.13560(120)	1.14(11)
O 2	0.40191(99)	0.35875(65)	0.26502(121)	1.18(11)
O 3	0.34456(94)	0.52995(57)	0.29881(139)	1.35(12)
O 4	0.73283(95)	0.57700(58)	0.50477(141)	1.57(15)
O 5	0.59977(119)	0.63990(72)	0.17052(183)	1.29(14)
O 6	0.88067(79)	0.55533(49)	0.29494(120)	1.26(13)
O 7	0.67354(78)	0.46506(48)	0.20091(112)	1.94(13)
O 8	0.60037(95)	0.83471(58)	0.24654(140)	1.51(12)
O 9	0.60012(93)	0.00046(56)	0.29928(111)	1.57(12)
O 10	0.80172(71)	0.90022(44)	0.19059(105)	1.44(12)
O 11	0.20706(93)	0.10629(58)	0.43929(129)	1.30(11)
O 12	0.44704(93)	0.15462(58)	0.27408(128)	1.58(12)
O 13	0.69893(92)	0.11796(57)	0.19834(126)	1.46(12)
O 14	0.71489(86)	0.11252(49)	0.56477(122)	1.84(13)
O 15	0.65205(76)	0.27387(47)	0.13538(121)	1.35(12)
O 16	0.93578(95)	0.18125(58)	0.29619(141)	1.58(12)
O 17	0.22355(75)	0.83779(46)	0.07440(120)	1.48(12)
O 18	0.85352(91)	0.72919(56)	0.11145(135)	1.26(11)
O 19	0.06830(94)	0.80492(57)	0.27437(139)	1.62(12)
O 20	0.34777(91)	0.71819(56)	0.34867(134)	1.42(12)
O 21	0.14822(90)	0.27164(56)	0.37394(134)	1.18(11)
O 22	0.09514(92)	0.15516(56)	0.08265(124)	1.38(12)
OH	0.88014(71)	0.35558(45)	0.03173(106)	1.51(21)
F	0.11449(73)	0.63584(44)	0.46082(105)	2.81(18)
W	0.0	0.0	0.0	7.07(99)

DISCUSSION

The crystal structure of miserite is controlled by the nature and linkages of chains composed of silica tetrahedra. There are two crystallographically independent sub-chains in the cell, each extending parallel to *c*. These sub-chains are linked together into Si_6O_{18} double chains across a pseudo-mirror plane in *ac*. Operation of the $\bar{1}$ symmetry of the space group produces a closed quadruple $\text{Si}_{12}\text{O}_{30}$ composite chain, with the *c* axis as its central axis, in which all tetrahedra share three corners. This type of chain linkage was previously unobserved (Clark 1972, p. 114). Its inter-tetrahedral Si-O-Si bond angles are listed in Table 9. The deviations of the composite chain from ideal *mmm* symmetry are slight, not exceeding 0.15 \AA . The three-member repeat unit of a single sub-chain is indeed similar to that of wollastonite; however, when the orientations of the tetrahedra are considered, it much more closely resembles that of pectolite (Prewitt & Buerger 1963, fig. 5).

The pipe-like nature of the eight-membered ring of the composite chain is clearly visible in *c*-axis projection at each corner of the cell (Fig. 1). In *b*-axis projection (Fig. 2), pipes adjacent along *a* are seen to be displaced vertically by exactly *c*/2, producing the large β angle of the cell. Such a pair of pipes is cross-linked by 9-coordinate K atoms, each of which is bonded to six O atoms of the pipe in which it lies and to three O atoms in the pipe adjacent along *a* (Fig. 2). The perfect {010} cleavage of miserite therefore must cut only four K-O and two Si-O bonds per cell, in general travelling through the void space of the pipes (Fig. 1). The {100} cleavage, although it can also pass through the pipes, requires the cutting of four Si-O, three Ca-O and three X-O bonds per cell; it tends therefore to proceed stepwise, alternating along both directions, resulting in its somewhat imperfect and frequently stepped character. The reason for the total absence of any other cleavage or parting direction is also clear from Figure 1.

this chain. Site refinements for O(H) and F showed that each was fully occupied and that there was little, if any, exchange.

The final *R* for 2755 observed reflections was 0.062. For all data, *R* was 0.071, with none of the unobserved reflections calculating at greater than 1.5 times its input value. Throughout the refinement Finger's (1969) least-squares program RFINE was used, with bond length and angle errors calculated by his linking program BADTEA. Atomic scattering factors used were those given by Cromer & Mann (1968) for ionized atoms, together with the anomalous dispersion coefficients of Cromer (1965). Final atomic coordinates are given in Table 6, and

*This table is available, at a nominal charge, from the Depository of Unpublished Data, CISTI, National Research Council of Canada, Ottawa, Canada, K1A 0S2.

TABLE 7. ANISOTROPIC THERMAL PARAMETERS ($\times 10^5$) FOR MISERITE

Site	β_{11}	β_{22}	β_{33}	β_{12}	β_{13}	β_{23}
Z	133(40)	139(18)	623(95)	21(23)	-117(53)	-31(34)
K	472(24)	151(9)	691(57)	-46(12)	226(29)	-15(17)
X	523(15)	185(6)	787(36)	-104(8)	78(18)	104(10)
Ca 1	220(21)	131(8)	477(33)	-20(10)	-146(24)	139(15)
Ca 2	306(21)	81(8)	358(50)	-45(10)	69(25)	94(14)
Ca 3	353(22)	172(9)	405(55)	-117(12)	78(26)	80(16)
Ca 4	345(21)	58(8)	696(54)	-45(10)	105(26)	50(15)
Ca 5	373(22)	136(9)	407(52)	-108(11)	3(26)	94(15)
Si 1	232(26)	117(11)	157(66)	-61(14)	-29(30)	69(19)
Si 2	232(27)	85(10)	253(66)	21(13)	8(31)	91(19)
Si 3	305(28)	73(10)	229(63)	-16(14)	85(31)	77(18)
Si 4	232(26)	70(10)	330(63)	-23(13)	16(30)	65(19)
Si 5	142(25)	94(10)	345(69)	-23(13)	46(30)	68(19)
Si 6	242(27)	147(11)	106(62)	-49(14)	37(30)	-18(19)
Si 7	180(25)	117(10)	185(66)	-22(13)	-6(30)	46(19)
Si 8	325(28)	96(10)	129(62)	-124(14)	93(31)	-8(19)
O 4	548(76)	157(27)	600(162)	-44(57)	145(88)	-1(48)
OH	387(80)	167(31)	864(192)	-19(40)	214(96)	107(57)
F	831(83)	263(29)	1509(187)	-163(39)	224(97)	-17(55)
W	2397(619)	479(163)	3736(1149)	55(253)	831(667)	-11(350)

Two side views of a single pipe, in each case normal to one of the vertical pseudo-mirror planes, are shown in Figure 3. The *xz* view presents a series of alternating four- and six-membered rings of tetrahedra, shown paired across a pseudo-mirror plane. In the *yz* view one

sees an eight-membered repeating unit, similarly paired across a second pseudo-mirror plane. The K atoms seen to lie within the pipe in *c*-axis projection (Fig. 1) in fact occupy the eight-membered rings of Figure 3, in effect functioning as part of the pipe wall. The geometric

TABLE 8. INTERATOMIC DISTANCES AND POLYHEDRAL ANGLES IN MISERITE

Distance (Å)		Angle		Opposite Edge (Å)	Distance (Å)		Angle		Opposite Edge (Å)
X-O(1)	2.440	O(1)-X-O(1)'	73.8°	2.817	Ca(4)-OH	2.302	O(4)-Ca(4)-O(6)	98.3°	3.822
-O(1)'	2.248	-O(6)	84.6	3.148	-F	2.406	-O(6)'	56.9	2.460
-O(6)	2.231	-OH	93.7	3.442	mean	2.444	-O(21)	73.0	2.866
-O(18)	2.227	-F	101.0	3.596			-OH	131.0	4.431
-OH	2.277	O(1)'-X-O(6)	89.5	3.151			-F	119.8	4.302
-F	2.217	-O(18)	95.1	3.249			O(6)-Ca(4)-O(6)'	86.1	3.472
mean	2.273	-OH	83.7	3.019			-OH	95.7	3.552
		O(6)-X-O(18)	89.7	3.143			-F	98.5	3.704
		-F	77.3	2.778			O(6)'-Ca(4)-O(21)	93.1	3.515
		O(18)-X-OH	90.5	3.198			-F	67.3	2.778
		-F	90.5	3.155			O(21)-Ca(4)-OH	86.6	3.106
		OH-X-F	109.6	3.672			-F	90.4	3.290
		mean	89.7				OH-Ca(4)-F	104.1	3.712
							mean	90.0	
Ca(1)-O(2)	2.532	O(2)-Ca(1)-O(4)	59.3	2.534	Ca(5)-O(2)	2.402	O(2)-Ca(5)-O(3)	105.9	3.871
-O(4)	2.592	-O(5)	107.4	4.168	-O(3)	2.449	-O(7)	106.1	3.733
-O(5)	2.640	-O(12)	80.1	3.199	-O(7)	2.267	-O(15)	75.6	3.000
-O(8)	2.486	-O(20)	79.6	3.189	-O(15)	2.491	-O(20)	81.0	3.189
-O(12)	2.439	-O(21)	92.8	3.543	-O(20)	2.506	O(3)-Ca(5)-O(7)	105.3	3.752
-O(20)	2.449	O(4)-Ca(1)-O(5)	58.0	2.557	-O(20)	2.218	-O(20)	74.6	3.002
-O(21)	2.358	-O(8)	122.4	4.450	mean	2.389	-F	82.1	3.069
mean	2.528	-O(12)	133.5	4.623			O(7)-Ca(5)-O(15)	80.9	3.091
		-O(20)	99.6	3.851			-F	83.2	2.977
		-O(21)	70.6	2.866			O(15)-Ca(5)-O(20)	98.8	3.793
		O(5)-Ca(1)-O(8)	74.6	3.108			-F	95.0	3.476
		-O(20)	78.3	3.215			O(20)-Ca(5)-F	89.3	3.327
		-O(21)	97.8	3.771			mean	89.8	
		O(8)-Ca(1)-O(12)	98.0	3.717	Si(1)-O(1)	1.632	O(1)-Si(1)-O(2)	114.1	2.732
		-O(20)	100.9	3.804	-O(2)	1.624	-O(3)	109.6	2.654
		-O(21)	86.9	3.334	-O(3)	1.617	-O(4)	103.2	2.557
		O(12)-Ca(1)-O(20)	93.7	3.567	-O(4)	1.631	O(2)-Si(1)-O(3)	110.9	2.670
		-O(21)	91.6	3.439	mean	1.626	-O(4)	102.3	2.534
		mean	90.3				O(3)-Si(1)-O(4)	116.6	2.764
Ca(2)-O(2)	2.295	O(2)-Ca(2)-O(5)	89.8	3.209			mean	109.5	2.652
-O(5)	2.253	-O(12)	83.7	3.199	Si(2)-O(4)	1.611	O(4)-Si(2)-O(5)	104.2	2.537
-O(8)	2.314	-O(15)	80.1	3.000	-O(5)	1.604	-O(6)	98.4	2.460
-O(12)	2.494	-O(18)	94.2	3.464	-O(6)	1.640	-O(7)	113.0	2.689
-O(15)	2.366	O(5)-Ca(2)-O(8)	85.8	3.108	-O(7)	1.613	O(5)-Si(2)-O(6)	113.2	2.709
-O(18)	2.432	-O(15)	77.7	2.897	mean	1.617	-O(7)	116.6	2.738
mean	2.359	-O(18)	92.4	3.584			O(6)-Si(2)-O(7)	109.8	2.661
		O(8)-Ca(2)-O(12)	101.1	3.714			mean	109.2	2.632
		-O(15)	102.1	3.639	Si(3)-O(8)*	1.603	O(8)-Si(3)-O(9)	110.0	2.639
		-O(18)	82.7	3.137	-O(9)	1.620	-O(10)	109.3	2.646
		O(12)-Ca(2)-O(15)	94.7	3.576	-O(10)	1.641	-O(11)	111.6	2.676
		-O(18)	94.6	3.619	-O(11)	1.633	O(9)-Si(3)-O(10)	104.3	2.575
		mean	89.9		mean	1.624	-O(11)	107.9	2.630
Ca(3)-O(3)	2.334	O(3)-Ca(3)-O(5)	111.1	3.858			O(10)-Si(3)-O(11)	113.5	2.739
-O(5)	2.345	-O(7)	104.0	3.634			mean	109.4	2.651
-O(7)	2.279	-O(20)	77.7	3.002	Si(4)-O(9)	1.668	O(9)-Si(4)-O(12)	103.6	2.577
-O(15)	2.430	-OH	84.9	3.087	-O(12)*	1.611	-O(13)	105.0	2.610
-O(20)	2.449	O(5)-Ca(3)-O(7)	105.9	3.691	-O(13)	1.621	-O(14)	105.9	2.635
-OH	2.241	-O(15)	74.7	2.897	-O(14)	1.634	O(12)-Si(4)-O(13)	114.4	2.718
mean	2.346	-O(20)	84.2	3.215	mean	1.634	-O(14)	117.1	2.768
		O(7)-Ca(3)-O(15)	82.0	3.091			O(13)-Si(4)-O(14)	109.6	2.659
		-OH	81.3	2.945			mean	109.3	2.661
		O(15)-Ca(3)-O(20)	94.7	3.588	Si(5)-O(13)	1.615	O(13)-Si(5)-O(15)	102.2	2.495
		-OH	87.7	3.240	-O(15)*	1.592	-O(16)	108.6	2.644
		O(20)-Ca(3)-OH	86.9	3.230	-O(16)	1.641	-O(17)	108.1	2.622
		mean	89.6		-O(17)	1.625	O(15)-Si(5)-O(16)	119.3	2.790
Ca(4)-O(1)	2.521	O(1)-Ca(4)-O(4)	60.3	2.557	mean	1.618	-O(17)	109.6	2.629
-O(4)	2.567	-O(6)	77.9	3.148					
-O(6)	2.484	-O(6)'	111.3	4.230					
-O(6)'	2.601	-O(21)	93.1	3.453					
-O(21)	2.227	-OH	77.4	3.019					

CONTINUED ON FOLLOWING PAGE

TABLE 8, CONTINUED

Distance (Å)		Angle	Opposite Edge (Å)	Distance (Å)		Angle	Opposite Edge (Å)
	O(16)-Si(5)-O(17)	108.5	2.650		O(21)-Si(8)-O(22)	111.4	2.669
	mean	109.4	2.638		mean	109.4	2.630
Si(6)-O(10)	1.635	O(10)-Si(6)-O(18)	114.0	2.711	K-O(8)	3.252	
-O(18)*	1.598	-O(19)	108.3	2.660	-O(9)	2.663	
-O(19)	1.647	-O(22)	107.1	2.608	-O(10)	3.000	
-O(22)	1.607	O(18)-Si(6)-O(19)	105.1	2.576	-O(11)	2.958	
mean	1.622	-O(22)	115.2	2.706	-O(12)	3.051	
		O(19)-Si(6)-O(22)	106.7	2.612	-O(13)	2.986	
		mean	109.4	2.646	-O(14)	2.948	
Si(7)-O(14)	1.640	O(14)-Si(7)-O(17)	104.1	2.582	-O(17)	2.806	
-O(17)	1.635	-O(19)	107.7	2.659	-O(22)	2.980	
-O(19)	1.653	-O(20)	111.5	2.695	-W	2.996	
-O(20)*	1.620	O(17)-Si(7)-O(19)	108.7	2.672	mean	2.962	
mean	1.637	-O(20)	111.7	2.693	Z-O(10)	3.007	
		O(19)-Si(7)-O(20)	112.8	2.726	-O(11)	3.158	
		mean	109.4	2.671	-O(13)	3.340	
Si(8)-O(11)	1.596	O(11)-Si(8)-O(16)	107.6	2.594	-O(14)	3.187	
-O(16)	1.619	-O(21)	109.8	2.635	-O(16)	3.241	
-O(21)*	1.625	-O(22)	108.1	2.592	-O(19)	3.416	
-O(22)	1.606	O(16)-Si(8)-O(21)	113.9	2.720	mean	3.225	
mean	1.612	-O(22)	105.8	2.572			

Notes: (1) The errors are 0.009Å for interatomic distances and 0.4° for polyhedral angles.

(2) O(1)' is (-x, -y + 1, -z) of O(1); O(6)' is (-x - 1, -y, -z) of O(6).

(3) The shortest O-O bond in any polyhedron is 2.460Å, between O(4) and O(6).

(4) Since the Z site is at a centre of symmetry, all Z-O distances occur twice.

(5) The Si(1) and Si(2) polyhedra form the Si₂O₇ group.

(6) An asterisk (*) indicates an oxygen not bonded to another silica tetrahedron in the composite chain.

centre of each ring pair corresponds to an inversion centre—to the origin (*W* site) in the four- and eight-membered rings, and to 0,0,½ (*Z* site) in the six-membered ring. These two sites are ideally empty, but since the minimum free-travel radius of the pipes is approximately 2.8Å, these sites are able to accept zeolitically-sorbed water and K/Ca, respectively. In the refined structure, zeolitic water half-occupies the *W* site and is relatively strongly held by two bonds to K atoms (Fig. 2). Given that the average rms thermal amplitude for this site is 0.3Å, the H atoms of the water molecules are undoubtedly disordered. If analyses of miserite from different localities are converted to atoms (on the basis of the data given in Table 3), it is seen (Table 4) that there is always an excess of K and Ca over their ideal values of 2 and 10 atoms, respectively. The 12-coordinate *Z* site, at 0,0,½, is statistically occupied by all excess K and part of the Ca, with an average bond length to the pipe tetrahedra of 3.22Å. Inclusion of this site in bond-valence calculations heavily oversaturates the bonding pipe oxygens, but if this site is omitted from the calculation, these oxygens resume their expected value of 2. Therefore, it is suggested that this *Z* site is ideally empty, that it is non-essential to the miserite structural framework, and that it zeolitically sorbs the excess K present in all miserite analyses.

A unique feature of the miserite structure is the presence of a pair of independent Si₂O₇ groups, isolated from the composite chains. Each group lies near the centre of the cell and the two are related by the centre of symmetry at ½,½,½. In *c*-axis projection (Fig. 1), the two groups are seen in eclipsed conformation facing each other across the cell centre, forming two opposite corners of a narrow central channel.

The remainder of the cell is filled by columns of edge-sharing Ca polyhedra, linked both to the pipes and to the central Si₂O₇ groups. As a result of the operation of the symmetry centre at ½,½,½, there are only three unique column types per cell; the repeat units of these are shown in Figures 4a and 4b. Within any column, each Ca polyhedron shares an edge with the ones above, below, before and behind it. In addition, polyhedra about the 7-coordinate calciums, Ca(1) and Ca(4), each share a different pair of edges with a single Si₂O₇ group. This is illustrated for Ca(1) in Figure 4b. Because of these complex edge-sharing arrangements among the Ca polyhedra and Si₂O₇ groups, the central portions of cells adjacent along *a* and *c* form an infinite slab, parallel to the *ac* plane, which is linked to the silicon pipes and falls between them in the *b* direction.

The slab composed of the Ca polyhedra and Si₂O₇ groups forms a stable structural unit, the

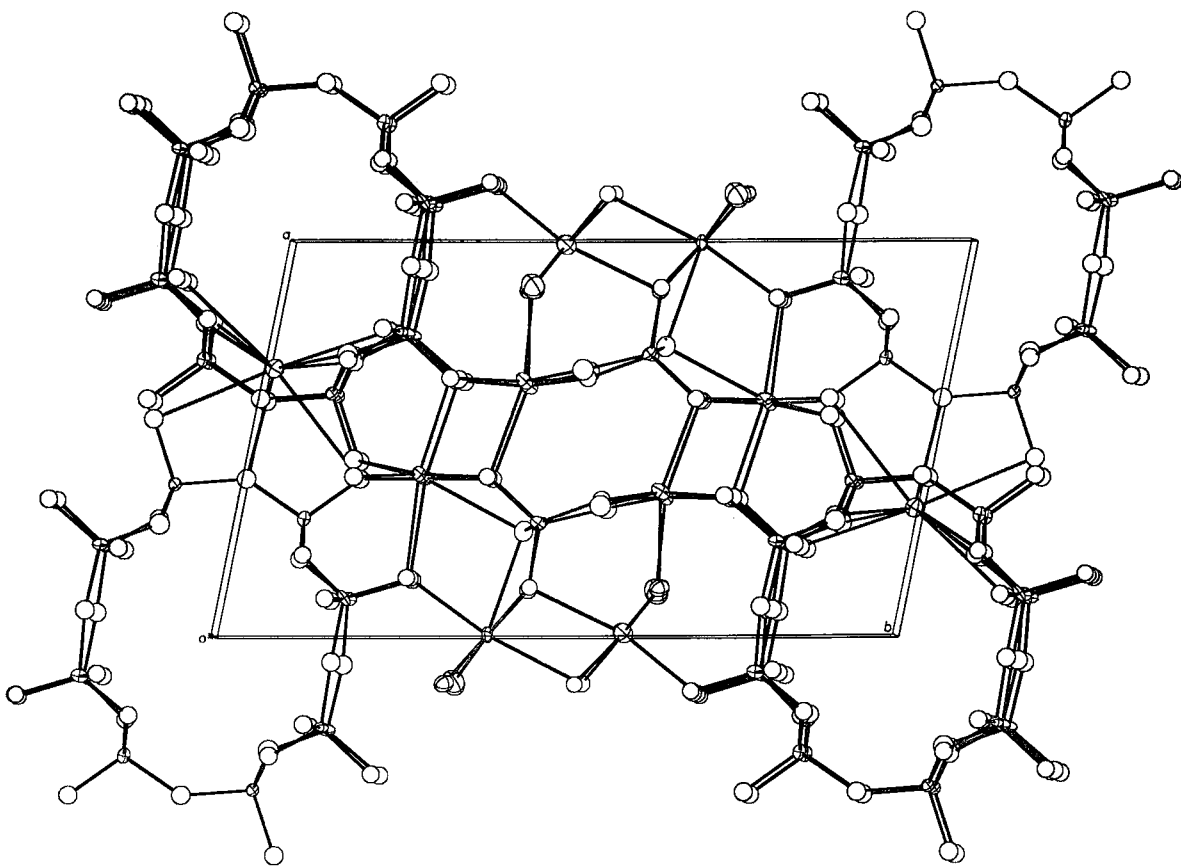


FIG. 1. Perspective view of the miserite structure in c -axis projection. Two chain composites of silica tetrahedra contain K atoms within the reference cell, and are here extended $\frac{1}{2}$ cell above and below the reference cell in order to emphasize their pipe-like nature (upper left and lower right corners). Note that the K atoms project inside the pipe boundaries and in effect form part of the pipe wall. A channel in the centre of the cell is defined by Si_2O_7 groups (half visible at upper right and lower left corners of the channel). The O(H) and F atoms, distinguished by their large anisotropic thermal ellipsoids, form two columns within the cell, each situated between a K-containing chain composite and an Si_2O_7 group.

anion matrix of which defines one 6-coordinate virtual cation site per asymmetric unit. This site, the X site, lies immediately adjacent to a somewhat sinuous open channel (radius $\approx 2.5\text{\AA}$) roughly parallel to c , between the Si_2O_7 groups in the centre of the cell (Figs. 1, 4b, 4c). In the Kipawa miserite, this site is fully occupied by rare earths plus other minor species, as shown by the successful refinement of its site occupancy using a composite scattering-factor curve; site occupancy refinements also show that all Ca sites in the slab are fully occupied by Ca.

The O(H) and F atoms form one edge of each Ca(4) polyhedron, and hence serve to define one edge of the octahedron about each virtual X site. Thus the O(H) and F sites alternate with approximately equal spacing to

form linear columns parallel to c (Figs. 4a, 4d). Each column is near the centre of what would otherwise be a roughly pentagonal open channel (Fig. 1) and bonds across this channel to Ca(3) (with O(H)) and Ca(5) (with F). Within the columns the O(H) and F sites are ordered and fully occupied. Either site has the potential to form an O-H-O or F-H-O bond, approximately 3\AA long, to any one of several O atoms belonging to either the Si_2O_7 groups or the main pipe walls. Interestingly enough, the oxygens with such bond-forming potential are the most undersaturated in bond-valence calculations; however, attempts to locate specific H sites on the final difference map were unsuccessful. The F atom has the highest isotropic temperature factor of any slab site; at 2.8\AA^2 it is almost

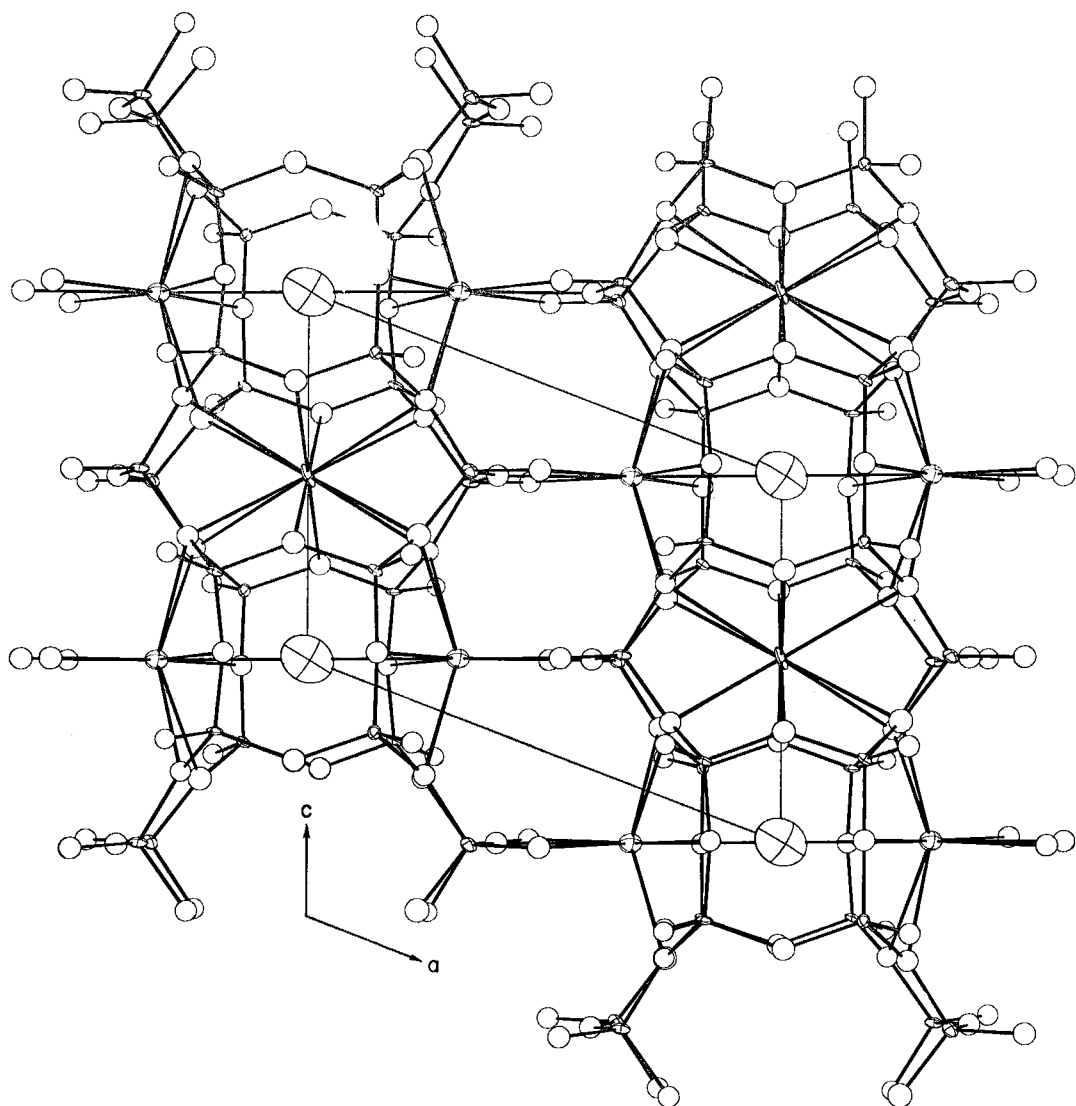


FIG. 2. Perspective projection of one end of the miserite cell normal to the ac plane, showing how the composite chains are cross-linked by K atoms lying between them in this plane. The W $(0,0,0)$ and Z $(0,0,\frac{1}{2})$ sites within the pipes are illustrated with their coordinations to indicate how filling these sites can block the pipes and why the W site is restricted to anions. Note that $K-W-K-Z-K \dots$ forms a nearly perfect horizontal plane across this projection, determining the vertical shift of $c/2$ between adjacent pipes and thus the β angle of the cell.

twice the value of 1.5 found for the O(H) site. Moreover, its anisotropic ellipsoid is elongated in the direction of the shortest F-O distance, possibly indicating a potential [O(H),F]-H bond.

There is no detectable O(H)-F interchange in the Kipawa miserite, although the possibility of a more hydroxyl-rich variety obviously exists; for example, the Central Asian analysis shows $(OH_{3.15}, F_{0.85})$ in the cell. Unfortunately, because of the structural geometry of the O(H) and F

sites, conventional thermogravimetric analyses for O(H) in miserite would automatically expel both O(H) and F simultaneously from their sites, yielding meaningless values for O(H) unless the total F content had already been determined by other methods, as in the present study. Thus reported values for O(H) and F in miserite from other localities are likely to be unreliable, especially in the case of the very high F content for miserite from the Talassk

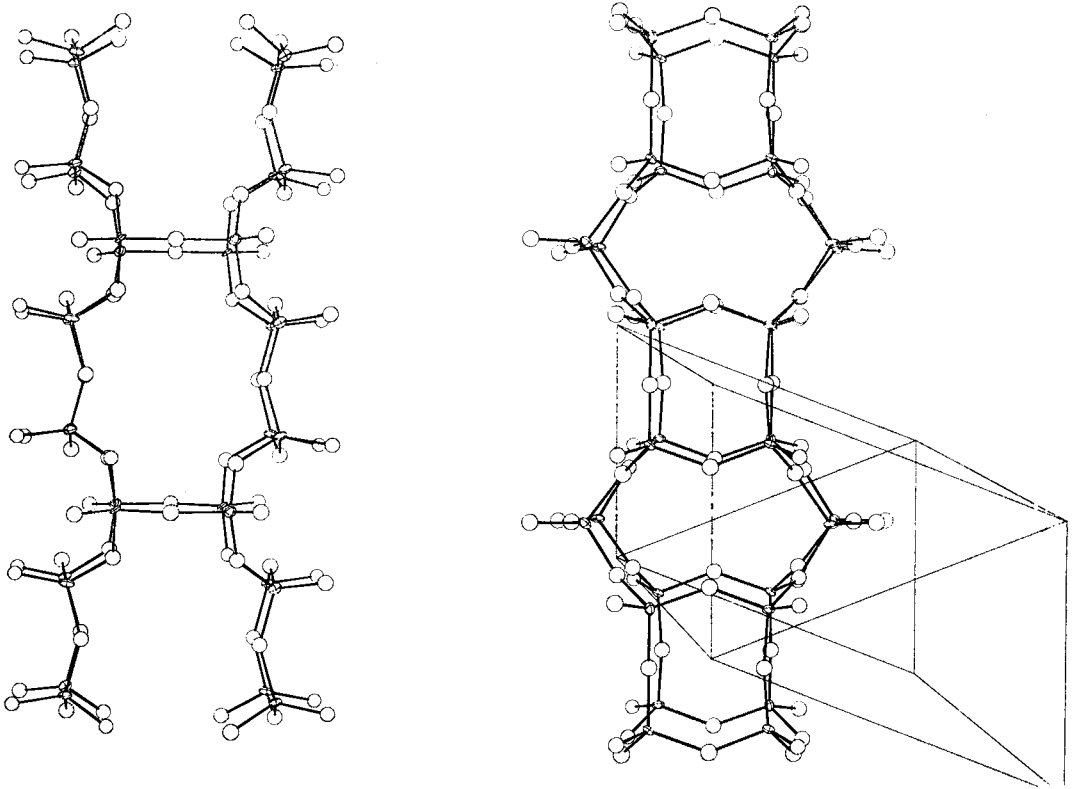


FIG. 3. The perspective view to the left, of one chain composite of silica tetrahedra in yz projection normal to one of the pseudo-mirror planes of the pipe, shows the 8-membered ring pairs. To the right is an xz projection of the same pipe, obtained by rotating the first by 90° around its vertical axis. The unit cell is outlined to distinguish the three-member repeat unit of an individual chain within the composite. The origin falls at the geometric centre of the 4-membered ring pairs. Note that the $[101]$ face diagonals of the cell correspond exactly in length with $[100]$.

Range (Table 4).

The miserite structure is a pyroxenoid derivative, the structural framework of which is described by the ideal formula $KCa_5(Si_8O_7)(Si_6O_{15})(OH)F$ ($Z=2$). As has been shown, these major elements form a complete, self-consistent framework of slabs and pipes, which defines three types of virtual site. Given that all available analyses of miserite from various localities (Table 4) show a large number of minor cations, including excess K and Ca, which are non-essential to the structure, and given also that there is virtually no replacement in the structural framework itself, it may be presumed that these minor cations form in effect a variable pool from which material may be statistically distributed among the virtual sites of a particular crystal. One of these sites, the W site, is restricted to occupancy by anions because it lies between two K atoms which are capable of forming relatively strong bonds to

the site. In the Kipawa miserite, the W site was found to be half-occupied by zeolitic H_2O ; it has, however, equal potential for holding F or variable amounts of F and H_2O . Analogous restrictions require the X and Z sites to accept only cations.

All the virtual sites are significantly easy of access, the W and Z sites via the large straight corner pipes, and the X site via the narrower sinuous central channel. Excess K, found in all existing analyses, is constrained by its size and bonding properties to enter only the Z site, but a cation of too small radius to form stabilizing bonds to the walls of the pipe at the Z site could nonetheless be trapped in a vacant X site while moving down one of the central channels. The miserite structure, in effect, functions as a kind of atomic sieve, accepting and, by the different natures of the virtual sites, potentially sorting the minor elements which percolate through it. For example, the X site in

the Kipawa miserite studied has been preferentially filled with yttrium and other minor species to the exclusion of Ca—the Kipawa carbonatite is known to display a local excess of rare-earth elements (Aarden & Gittins 1974); in this case all excess Ca occupies the Z site.

The average X-anion bond length in the Kipawa miserite is 2.273 Å, almost the same as the Y-O bond length in Y_2O_3 , and considerably shorter than the average Ca-O bond length (2.413 Å) of the Ca polyhedra.

Tentative site occupancies for other miserite

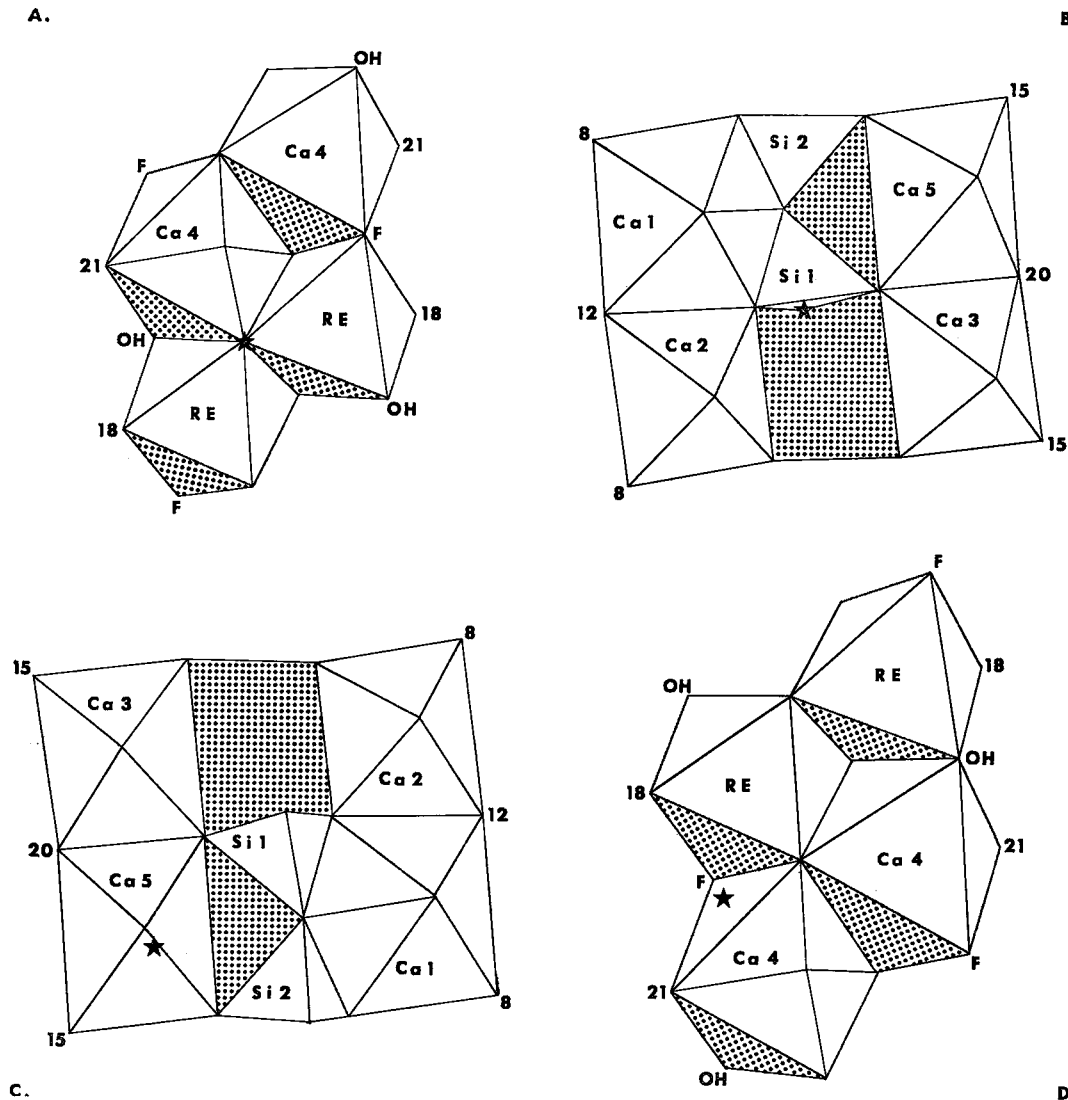


FIG. 4. The repeat units of the polyhedral columns of the slabs are shown by a series of perspective slices through the central portion of the structure, with z vertical and y horizontal, proceeding from one side of the cell to the other along a . The centre of symmetry at $\frac{1}{2}, \frac{1}{2}, \frac{1}{2}$ is located between 4B and 4C. In 4A and 4D, centres of symmetry are located at the midpoints of the shared edges between equivalent polyhedra. Note that the Si_2O_7 groups share two different pairs of edges with the two seven-coordinate Ca polyhedra; for example, the Si_2O_7 group sharing edges with the Ca(1) polyhedron in 4B also shares its hidden edge-pair with the apex of the Ca(4) polyhedron to the left in 4A. The stars indicate the line of projection of the slices, running through O(1) in 4A and 4B, and passing close to F ($-x, -y, -z$) in 4C and 4D. Numbered sites are for non-bridging oxygens of the composite chains. The shaded areas of 4B and 4C indicate the central empty channel. Access from this channel to the RE site is particularly easy, since the Ca(2) octahedron of 4B is completed by O(18) and the Ca(3) octahedron of 4B by OH.

analyses are given in Table 4. These show that the *X* site is generally fully occupied, whereas the *Z* site is not. A cation filling an *X* site is strongly held within an anion octahedron, but without blocking subsequent motion through the adjacent channel. Not only is a cation in a *Z* site weakly held, but also the free passage of cations through a pipe is hindered by filling either *Z* or *W* sites; addition of cations or anions to unfilled sites in a pipe therefore requires that local occupants must move to equivalent sites further along. The Russian analyses show a general deficiency in Si and extreme variability in F (Table 4). This, together with the large errors in the calculated cell volumes (Table 3), renders exact site assignments impossible for the Russian material. There is also a problem with the density reported for Yakutian miserite, which should more closely resemble that of the Kipawa miserite given the great similarity between analyses and cell dimensions. It is probable that digits have been transposed in the original paper, and that a correct reading is 2.873 rather than 2.783; such a revision results in a linear plot of density versus cell volume for the first four analyses of Table 3.

CONCLUSIONS

Earlier proposals of a structural similarity between miserite and xonotlite (e.g. Kupriyanova & Vasileva 1961) are now clearly demonstrated to be incorrect. The Si_6O_{17} double chain of xonotlite may be considered as two parallel wollastonite chains, cross-linked at every third tetrahedron, with a 2-fold axis passing through the bridging oxygens (Dent & Taylor 1956). The analogous situation in miserite (Fig. 3, *yz* view) has a pseudo-mirror plane replacing the 2-fold axis such that even the half-pipe tetrahedra do not have the xonotlite orientation; moreover, in xonotlite all inter-tetrahedral angles are approximately 158° , much larger than those of miserite. Finally, in the xonotlite structure, the $[\text{CaO}_6]_\infty$ polyhedral columns are arranged in linear edge-sharing triplets, an octahedral column sandwiched between two columns of trigonal prisms, resulting in a strong pseudo-period of $b/2=3.66\text{\AA}$ for the fibre axis which is typical of all xonotlite derivatives. Such a pseudo-period is not present in miserite, and the arrangement of Ca polyhedra found in it is totally unlike that of xonotlite.

Miserite bears no simple structural relationship to any other known silicate. The basic three-member repeat unit of a single chain within a pipe-composite is clearly of pyroxenoid type, the chain direction in the cell showing the period of approximately 7.3\AA typical of such

structures. As noted previously, the similarity of a single chain is closer to the chain found in pectolite than to that of wollastonite. The inter-tetrahedral angles for the pectolite chain are 135.0° – 147.8° – 136.4° and the corresponding angles for chain II of miserite (Table 9) are

TABLE 9. INTERTETRAHEDRAL ANGLES IN MISERITE

Tetrahedron Pair	Angle	Affiliation
Si(1)-O(4)-Si(2)	151.5°	Si ₂ O ₇ group
Si(3)-O(9)-Si(4)	141.0	interchain link in <i>yz</i>
Si(3)-O(10)-Si(6)	131.0	chain I*
Si(3)-O(11)-Si(8)	137.2	chain I
Si(4)-O(13)-Si(5)	143.1	chain II**
Si(4)-O(14)-Si(7)	135.9	chain II
Si(5)-O(17)-Si(7)	149.6	chain II
Si(5)-O(16)-Si(8)	140.4	interchain link in <i>xz</i>
Si(6)-O(19)-Si(7)	140.2	interchain link in <i>xz</i>
Si(6)-O(22)-Si(8)	149.6	chain I

* Si(7)-Si(4)-Si(5) repeat unit

**Si(6)-Si(3)-Si(8) repeat unit

131.0° – 149.6° – 137.2° , whereas wollastonite has the angles 140° – 149° – 139° . The presence of four such chains, related by pseudo *mm* symmetry about the pipe axis, and in which all tetrahedra share three corners, is, however, unique. Addition of the isolated Si₂O₇ groups clearly removes the structure from Zoltai Type 2e (multiple chains), where it would otherwise have been the only member, to become the first known structure to occupy Zoltai Type 5 (mixed types) (Zoltai 1960).

ACKNOWLEDGEMENTS

Microprobe analyses were made by Dr. M. I. Corlett, and fluorine analyses by Mr. S. Haynes, graduate student, using his newly-developed technique, in the Department of Geological Sciences at Queen's University. Thanks are due to Dr. S. Guggenheim of the University of Wisconsin-Madison for providing unpublished data on miserite from Wisconsin. The analytical data for Arkansas miserite of Dr. C. Milton of George Washington University were communicated to Dr. L. G. Berry, and are used with his permission. Many crystallographers generously made available computer programs, some still in developmental stages, during the search for a suitable trial model of the miserite structure. Special thanks are expressed to Miss M. E. Mrose of the U.S. Geological Survey for encouragement and stimulating discussions.

Extensive technical editing was done by Mrs. D. L. Scott of the Department of English, Queen's University, who superintended the manuscript through numerous revisions.

The author deeply appreciates the encouragement and assistance of Dr. L. G. Berry, who initiated structural studies of miserite at Queen's University and displayed great patience through four years of painful trials. In particular he provided valuable assistance with problems relating to the pseudo-cell and in indexing the final photographs, as well as innumerable discussions while the work was in progress.

This study was supported by grants from the National Research Council of Canada made to Dr. L. G. Berry.

REFERENCES

- ALCOCK, N. W. (1970): The analytical method for absorption correction. In *Crystallographic Computing* (F. R. Ahmed, ed.). Munksgaard.
- AARDEN, H. M. & GITTINS, J. (1974): Hiortdahlite from Kipawa River, Villedieu Township, Temiscaming County, Quebec, Canada. *Can. Mineral.* 12, 241-247.
- ARKHANGEL'SKAYA, V. V. (1968): Albitized rare metal granite found for the first time in the Olekma-Vitim Highlands. *Dokl. Akad. Nauk SSSR* 183, 162-164.
- BERRY, L. G., LIN, H.-C. & DAVIS, G. C. (1971): A new occurrence of miserite from the Kipawa Lake area, Temiscamingue Co., Quebec. *Can. Mineral.* 11 (1972), 569 (Abstr.).
- CLARK, C. M., SMITH, D. K. & JOHNSON, G. G. (1975): A FORTRAN IV program for calculating x-ray powder diffraction patterns—Version 5. *Penn. State Univ. Dep. Geosci. Rep.*
- CLARK, G. M. (1972): *The Structures of Non-Molecular Solids: A Co-ordinated Polyhedron Approach*. Applied Science Publishers, London.
- CROMER D. T. (1965): Anomalous dispersion corrections computed from self-consistent field relativistic Dirac-Slater wave functions. *Acta Cryst.* 18, 17-23.
- & MANN, J. B. (1968): X-ray scattering factors computed from numerical Hartree-Fock wave functions. *Acta Cryst.* A24, 321-324.
- DENT, L. S. & TAYLOR, H. F. W. (1956): The dehydration of xonotlite. *Acta Cryst.* 9, 1002-1004.
- FINGER, L. W. (1969): RFINE. A Fortran IV computer program for structure factor calculation and least-squares refinement of crystal structures. *Geophys. Lab. Carnegie Inst. Wash.* (unpubl. manuscript).
- GERMAIN, G., MAIN, P. & WOOLFSON, M. M. (1971): The application of phase relationships to complex structures. III. The optimum use of phase relationships. *Acta Cryst.* A27, 368-376.
- HAMILTON, W. C., ROLLETT, J. S. & SPARKS, R. A. (1965): On the relative scaling of x-ray photographs. *Acta Cryst.* 18, 129-130.
- KOZLOVA, P. S. (1962): Miserite from the Talassk Range. *Trudy Mineral. Muz. Akad. Nauk SSSR* 13, 198-204 (in Russ.).
- KRAVCHENKO, S. M. & BYKOVA, A. V. (1967): Miserite from southern Yakutia. *Mineral.-Pegmatitov Gidroterm. Shchelochnykh Massivov. Akad. Nauk SSSR, I.M.G.R.E.* 160-167 (in Russ.).
- KUPRIYANOVA, I. I. & VASILEVA Z. V. (1961): On rare-earth miserite, more information about the mineralogy of deposits of rare elements. *Geol. Mestorozhd. Redk. Elementov* 9, 139-147 (in Russ.).
- PREWITT, C. T. & BUERGER, M. J. (1963): Comparison of the crystal structures of wollastonite and pectolite. *Mineral Soc. Amer. Spec. Pap.* 1, 293-302.
- RYZHOV, B. I. & MOLEVA, V. A. (1960): A discovery of miserite in the U.S.S.R. *Dokl. Akad. Nauk SSSR* 131, 396-397.
- SCHALLER, W. T. (1950): Miserite from Arkansas; a renaming of natroxonotlite. *Amer. Mineral.* 35, 911-921.
- ULYANOVA, T. P. & ILINSKI, G. A. (1964): New data on the Khodzhaachkan miserite (Alay Range). *Mineral. Geokhim. Leningrad Gos. Univ., Sb. Statei* 1, 40-46 (in Russ.).
- WILLIAMS, J. F. (1891): The igneous rocks of Arkansas. *Geol. Surv. Arkansas, Ann. Rep. for 1890*, 2, 358.
- ZOLTAI, T. (1960): Classification of silicates and other minerals with tetrahedral structures. *Amer. Mineral.* 45, 960-973.

Manuscript received March 1976, emended July 1976.